Journal of *Marine Science and Engineering*

MDPI

Article

Characterization of the Mitochondrial Genome, Ecological Distribution, and Morphological Features of the Marine Gastropod Mollusc *Lophocochlias parvissimus* (Gastropoda, Tornidae)

Minju Kim [1,2,†], Hyeongwoo Choi [3,†], Hyeon Kim [1,2], Jiwon Kang [3], Hyeon Gyeong Jeong [4], Seong-il Eyun [3,*] and Jung-Hoon Kang [1,2,*]

[1] Ecological Risk Research Department, Korea Institute of Ocean Science and Technology, Geoje 53201, Republic of Korea
[2] Department of Ocean Science, University of Science and Technology, Daejeon 34113, Republic of Korea
[3] Department of Life Science, Chung-Ang University, Seoul 06974, Republic of Korea
[4] Department of Taxonomy and Systematics, National Marine Biodiversity Institute of Korea, Seocheon 33662, Republic of Korea
* Correspondence: eyun@cau.ac.kr (S.-i.E.); jhkang@kiost.ac.kr (J.-H.K.)
† These authors contributed equally to this work.

Abstract: The larvae of the marine gastropod *Lophocochlias parvissimus* are meroplankton that spend part of their lives as plankton that disperse and drift in the water column before settling on the sea floor. Two individuals of *L. parvissimus* larvae were sampled by the Multiple Opening/Closing Net and Environmental Sensing System (MOCNESS) from the Central Indian Ridge of the southwestern Indian Ocean in 2018 and 2019. We generated the first mitochondrial sequences for *L. parvissimus*, which will provide valuable genetic insight into the evolution of these organisms. In this study, we have determined that the mitogenome of *L. parvissimus* was 13,575 bp in length, consisting of 13 protein-coding genes, 18 tRNAs, and two rRNAs. Our work provides a new insight into the dispersal of *L. parvissimus* and previously missing components to the general understanding of the evolution of Truncatelloidea (Subclass Caenogastropoda).

Keywords: marine microgastropod; mitochondrial genome; Onnuri Vent Field

Citation: Kim, M.; Choi, H.; Kim, H.; Kang, J.; Jeong, H.G.; Eyun, S.-i.; Kang, J.-H. Characterization of the Mitochondrial Genome, Ecological Distribution, and Morphological Features of the Marine Gastropod Mollusc *Lophocochlias parvissimus* (Gastropoda, Tornidae). *J. Mar. Sci. Eng.* **2023**, *11*, 2307. https://doi.org/10.3390/jmse11122307

Academic Editors: David Osca and Alexandre Lobo-da-Cunha

Received: 31 October 2023
Revised: 1 December 2023
Accepted: 2 December 2023
Published: 6 December 2023

1. Introduction

Meroplankton are larvae of benthic animals that spend part of their lives as plankton, and this phase in their lifecycle plays a critical role in dispersal distance [1]. Planktonic larvae are at the stage of being able to free swim, during which some species may feed, not only promoting dispersal but also colonization and resilience in the deep sea [2,3]. Meroplankton larvae may spend different temporal scales, from hours to weeks or months, in the phase of drifting and dispersing by the currents in the water column before settling and metamorphosing on the sea floor [4]. Meroplankton differ from holoplankton, which remain planktonic throughout their lives [5,6]. The distinct morphological features of gastropods are that the meroplankton of gastropods differ from holoplanktonic gastropods by their diamond-patterned shells with relatively large coils [5,6].

Lophocochlias parvissimus (Hedley, 1899), described as *Liotia parvissima* (Hedley, 1899), *Parviturbo parvissimus* (Hedley, 1899), and *Parviturboides parvissimus* (Hedley, 1899), has also appeared in the literature of Pilsbry (1921) as *Haplocochlias (Lophocochlias) minutissimus* [7,8]. The shell of *L. parvissimus* is small (diameter of 0.84 mm), solid, and turbinate, with a cream color, four whorls, and an umbilicus that is small, oblique, narrow, and deep [9]. *L. parvissimus* is commonly found in subtidal areas including the sediments of tide pools [10,11]. Small molluscs that are smaller in diameter than 10 mm are often in abundance and have

great diversity [12]. The larvae of *L. parvissimus* are planktotrophic, so they are free-living and feed in the water column [11]. *L. parvissimus* are distributed across the Indo-Pacific region, including Hawaii, the Cocos-Keeling Islands, the Kiribati Republic, Fanning Island, the Line Islands from Jordan, Mozambique, Madagascar, Reunion, New Caledonia, the Loyalty Islands, Vanuatu, Fiji, Papua New Guinea, the Philippines, French Polynesia, and Western Australia's tropical Kimberley region [12–16].

Tornidae is a family of small marine snails with operculum in the clade Littorinimorpha, including 30 genera [8]. The genus *Lophocochlias* has two species: *L. parvissimus* Hedley (1899) and *L. procerus* Rubio and Rolán (2015) [7,8,15]. These small molluscs are an important food source for benthic predators, and they are important grazers and bioturbators of sediments [12]. Most of the previous studies on *L. parvissimus* have focused on the adult species that live in the sediment or larvae in the coastal waters, so the dispersal and distribution of *L. parvissimus* in the larval stage in the open ocean have not yet been studied.

Mitochondria are characterized by unique features, including maternal inheritance, notable conservation, multiple copies within cells, a low sequence recombination rate, and a rapid evolutionary rate [17]. Due to these features, mitochondrial sequences are extensively utilized in phylogenetic research [18]. Compared to the other mitochondrial genes, cytochrome c oxidase subunit I (*COX1*) exhibits a more robust phylogenetic signal [19]. As of October 2023, despite their extensive use in various studies, no mitochondrial genome sequences from the family Tornidae had been publicly available. As mitochondrial genomes play a crucial role in phylogeny and evolutionary history, we generated mitochondrial genome sequences and assembled the mitochondrial genome of *L. parvissimus*. We present the first phylogenetic analysis to elucidate the evolutionary relationships of *L. parvissimus* within the family Tornidae.

2. Materials and Methods

Sample collection. The study was carried out in the water column above hydrothermal vent sites during 2018 and 2019, as part of the expedition conducted by the Korea Institute of Ocean Science and Technology (KIOST) to the Central Indian Ridge on board the R/V ISABU (Figure 1 and Table 1). All the samples were obtained from hydrothermal vents of the Onnuri Vent Field (OVF), Solitaire Field (SF), and Station A in June 2018 and OVF and Station B in July 2019 [5,20]. Stations A and B served as control sites in the northern region, outside the immediate influence of the hydrothermal vents. Site selection was informed by the direction of meridional Ekman flows, in which the water is transported from the northern area to the southern area during the boreal summer monsoon (Figure 1) [21].

Table 1. The sampling strata and the environmental factors, including temp. (°C): average temperature, sal.: average salinity, chl *a*: integrated chlorophyll-a (mg m^{-3}) concentrations, and total abundance of *Lophocochlias parvissimus* (ind. 100 m^{-3}) at the sampling stations during 2018 and 2019 in the Central Indian Ridge. N.S.: not sampled.

Station	Date, Time	Longitude (°E), Latitude (°S)	Bottom Depth (m)	Sampling Strata (m)	Temp. (°C)	Sal.	Chl *a* (mg m^{-3})	*Lophocochlias parvissimus* Larvae (ind. 100 m^{-3})
A	2018-06-26 02:40~07:11	67°10.45, 9°28.18	1429	(1) 0–100	25.3	34.8	N.S.	0.4
				(2) 100–200	15.8	35.0	N.S.	0
				(3) 200–400	11.8	34.9	N.S.	0
				(4) 400–600	8.6	34.7	N.S.	0
				(5) 600–800	7.3	34.7	N.S.	0
				(6) 800–1000	6.3	34.7	N.S.	0
				(7) 1000–1300	5.1	34.7	N.S.	0

Table 1. *Cont.*

Station	Date, Time	Longitude (°E), Latitude (°S)	Bottom Depth (m)	Sampling Strata (m)	Temp. (°C)	Sal.	Chl *a* (mg m^{-3})	*Lophocochlias parvissimus* Larvae (ind. 100 m^{-3})
Onnuri Vent Field	2018-06-24 04:25~09:07	66°24.42, 11°28.86	2374	(1) 0–200	22.0	35.0	13.5	0
				(2) 200–500	10.7	34.8	N.S.	0
				(3) 500–1000	6.9	34.7	N.S.	0
				(4) 1000–1300	4.9	34.7	N.S.	0
				(5) 1300–1600	3.8	34.7	N.S.	0
				(6) 1600–1900	3.0	34.7	N.S.	0
Onnuri Vent Field	2019-07-02 15:18~22:51	66°20.20, 11°20.61	2111	(1) 0–200	22.3	35.0	18.9	0.3
				(2) 200–400	11.9	34.6	N.S.	0
				(3) 400–700	8.2	34.7	N.S.	Tangled nets
				(4) 700–1000	6.2	34.7	N.S.	Tangled nets
				(5) 1000–1300	4.8	34.7	N.S.	Tangled nets
				(6) 1300–1600	3.8	34.5	N.S.	Tangled nets
				(7) 1600–1900	3.1	34.7	N.S.	0
B	2019-07-04 20:52~23:05	67°10.88, 9°21.38	2126	(1) 0–100	26.0	23.2	N.S.	0
				(2) 100–200	15.9	25.8	N.S.	Tangled nets
				(3) 200–300	12.5	26.5	N.S.	Tangled nets
				(4) 300–400	11.3	26.7	N.S.	0
				(5) 400–500	9.7	26.8	N.S.	Tangled nets

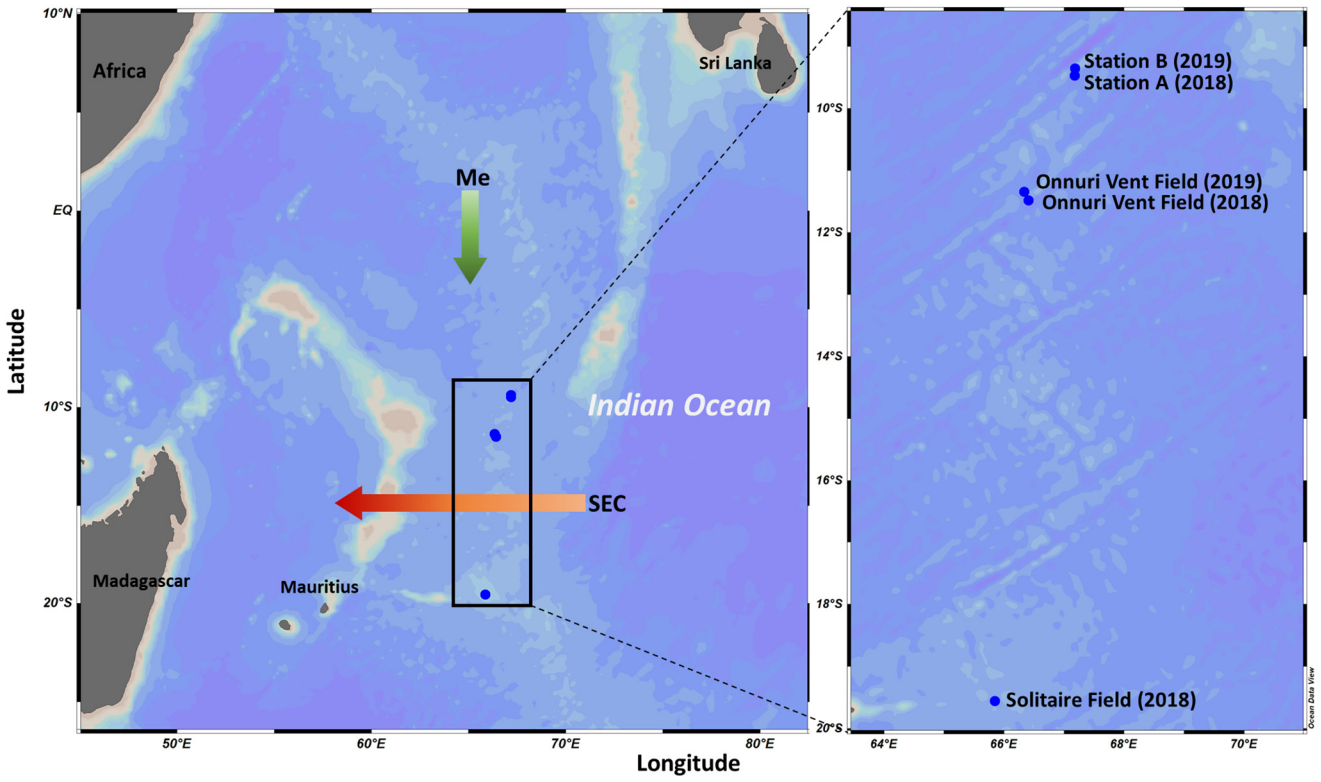

Figure 1. The survey stations at the Central Indian Ridge. South Equatorial Current (SEC) and the direction of meridional Ekman transport (Me) cited from Hood et al. (2017).

The physical properties of the sites were measured using sensors (Sea-bird Electronics, Bellevue, WA, USA) of conductivity, temperature, and depth. Sensors were attached to an environmental sensing and sample collection system that employs a network of mesh nets that can be opened or closed at the discretion of the operator in order to control the timing of collection and maintain sample quality (Multiple Opening/Closing Net and Environmental Sensing System, MOCNESS; Biological environmental sampling systems Inc., BESS, Falmouth, MA, USA). The seawater samples for the analysis of chlorophyll *a* (chl *a*) concentration were obtained using Niskin bottles (PVC) mounted on the Rosette sampler. The chl *a* concentration water samples were not collected at stations A and B due to limited sampling time. The analysis of chl *a* concentrations was carried out at 5 depths, including the layers of surface and subsurface chlorophyll maximum. Seawater samples were filtered (47 mm GF/F, Whatman, GE Healthcare, Marlborough, MA, USA) under low vacuum pressure (<125 mmHg). The GF/F filters were frozen (−80 °C) until the extraction of samples in acetone (90%) at 4 °C in the dark for two days. Chl *a* concentration was determined using a fluorometer that was calibrated using Turner Designs chl *a* standard solution (Turner Designs, San Jose, CA, USA), as described by Parsons et al. (1984) [22]. The chl *a* concentrations data were integrated for all depths from surface to 200 m.

The zooplankton samples, including *L. parvissimus* larvae, were collected with a MOCNESS equipped with 200 µm mesh nets. The sensors of pressure, conductivity, and temperature were mounted on MOCNESS (Sea-Bird Electronics, USA). The deep-tow winch was used to attach MOCNESS, and the winch wire speed during the pay-out and haul-in was 20–30 m min^{-1}. The vessel speed was kept between 1.5 and 2.0 knots during towing, and the net angle was maintained at the optimum angle of 45° for optimal sampling. Oblique tows after the deployment of MOCNESS to 100 m above the bottom were carried out to collect samples, and the sampling strata were divided into 5–7 layers (Table 1). The flowmeter attached to the MOCNESS was used to calculate the volume of filtered water. The MOCNESS sampling was successful in 2018. However, the process of collecting samples was more challenging in 2019, probably due to bad weather conditions that led to tangled nets at the depth layers 400–700 m, 700–1000 m, 1000–1300 m, and 1300–1600 m in the OVF (Table 1).

Zooplankton samples collected in cod-end buckets were transferred to sampling bottles that were further divided into two groups, in which one was fixed with borax-neutralized formalin (final concentration of 5%) for microscopic examination and the other sample was fixed with ethanol (99.9%) and was stored at –20 °C for further molecular analysis. Identification of *L. parvissimus* larvae was carried out under a stereomicroscope at 10×–80× magnification by isolating specimens with the same morphological features (Discovery V8, SteREO, Zeiss, Oberkochen, Germany). Photographs of the *L. parvissimus* samples were taken using a camera coupled to the stereoscope at 80× magnification (AxioCam ICc 3, Zeiss, Oberkochen, Germany). The total number of individuals was converted to individuals 100 m^{-3} (ind 100 m^{-3}). The larvae of *L. parvissimus* derived from the ethyl-alcohol samples were sorted by morphological characteristics that were previously stated by Hedley, 1899 [9]. The confirmation of the species identification was conducted using genomic DNA extraction methods.

Next-generation sequencing and mitochondrial genome assembly. Whole genomic DNA was extracted using a QIAGEN Blood & Cell Culture DNA Mini Kit (QIAGEN, Hilden, Germany), according to the manufacturer's instructions. Then, a 150 bp paired-end reads library was constructed using the TruSeq DNA Nano 550 bp kit (Illumina, Inc., San Diego, CA, USA) and sequenced with the Novaseq6000 platform (Illumina).

Quality control was performed using Trim Galore! (ver. 0.6.10) (https://www.bioinformatics.babraham.ac.uk/projects/trim_galore, accessed on 30 October 2023) with the following parameters [23,24]; -quality 20 -length 120 -max_n 0.

Then, we carried out de novo assembly using MitoZ (ver. 3.4) [25] to generate the mitochondrial genome sequence of *L. parvissimus*. Next, annotation of protein-coding genes (PCGs) was performed using the MITOS1 (http://mitos.bioinf.uni-leipzig.de/index.

py, accessed on 30 October 2023) and MITOS2 web servers () and visualized by Circos (ver. 0.69–8) [26].

Phylogenetic analysis. To delineate phylogenetic relationships, we utilized both the cytochrome c oxidase subunit I (COX1) gene and 13 protein-coding genes (PCGs). In the COX1 data, we used sequences from 16 species of Truncatelloidea obtained from the National Center for Biotechnology Information (NCBI) nucleotide database. *Haliotis discus hannai* was used as an outgroup species (Table 2). The multiple sequence alignments (MSA) were generated using MAFFT (ver. 7.475) [27]. To identify the best-fit evolutionary model, we used ModelFinder implemented in IQ-TREE (ver. 2.2.0.3) based on the Bayesian information criterion [28]. The COX1 dataset best fits the GTR + F + I + G4 evolutionary model.

Table 2. GenBank accession numbers of the cytochrome oxidase subunit 1 (COX1) from 17 gastropods.

Superfamily	Family	Species	Accession Number
Truncatelloidea	Tornidae	*Lophocochlias parvissimus*	OR343907
		Lophocochlias minutissimus	LC598190.1
		Pseudoliotia micans	KC439806.1
		Elachorbis subtatei	KC439807.1
	Cochliopidae	*Heleobia australis*	MT295126.1
		Helebops docimus	AF129322.1
		Juturnia kosteri	KF876283.1
		Littoridinops tenuipes	EF490566.1
	Iravadiidae	*Iravadia australis*	JX970607.1
		Iravadia resima	KC439779.1
	Caecidae	*Caecum japonicum*	LC598181.1
		Caecum trachea	KC439805.1
	Tateidae	*Sulawesidrobia bicolor*	HM587338.1
		Potamopyrgus antipodarum	MG979468.1
		Fluviopupa brevior	KC875085.1
		Tatea rufilabris	KC439802.1
Haliotoidea	Haliotidae	*Haliotis discus hannai*	JF748784.1

Within the 13 PCGs dataset, we concatenated 13 genes from seven mitochondrial genome sequences. Specifically, five sequences were derived from Littorinimorpha, while two were sourced from Neogastropoda and used as outgroups. The MSA for the 13 PCGs was performed utilizing MAFFT. Subsequently, the optimal partitioning scheme and best evolutionary models for each gene were determined using PartitionFinder (ver. 2.1.1) based on the Bayesian information criterion [29].

Maximum likelihood (ML) phylogeny tree was constructed using raxml-ng (ver. 0.9.0) [30]. Bayesian Inference (BI) tree was reconstructed using Mrbayes (ver. 3.2.4) [31]. We conducted 1000 bootstrap replicates in the ML analysis to ensure robustness and reliability. We employed two independent Markov chain Monte Carlo (MCMC) runs for the BI method, each comprising 1×10^6 generations. Sampling was performed every 500 generations, and an initial 25% of the samples were discarded as burn-in to ensure the convergence of the chains. The ML tree topology with bootstrapping support values (BS) from ML and Bayesian posterior probabilities (BPP) from BI on each node was visualized by FigTree (ver. 1.4.4) (http://tree.bio.ed.ac.uk/software/figtree, accessed on 30 October 2023).

3. Results and Discussion

Using MOCNESS sampling, a total of two representative *L. parvissimus* larvae were identified: one was retrieved from a depth of 0–100 m at Station A in 2018 and one from the 0–200 m depth range at OVF in 2019 (Figure 2). Small molluscs that are usually less than 10 mm in diameter are known to be important as a food source for benthic predators and also important grazers of sediments [12]. In this study, the two specimens of *L. parvissimus*

larvae had a mean diameter of 398.4 µm and a mean height of 356.3 µm (Figure 2). The distribution of *L. parvissimus* larvae, expressed in cubic meters, was 0.4 ind. 100 m^{-3} and 0.3 ind. 100 m^{-3} at Station A and OVF, respectively (Table 1). In the stations where *L. parvissimus* appeared, the average temperature and salinity were 25.3 °C and 34.8 for 0–100 m at Station A during 2018 and 22.3 °C and 35.0 for 0–200 m at OVF during 2019 (Table 1). The integrated chl *a* concentrations were 18.9 mg m^{-3} at OVF during 2019 (Table 1).

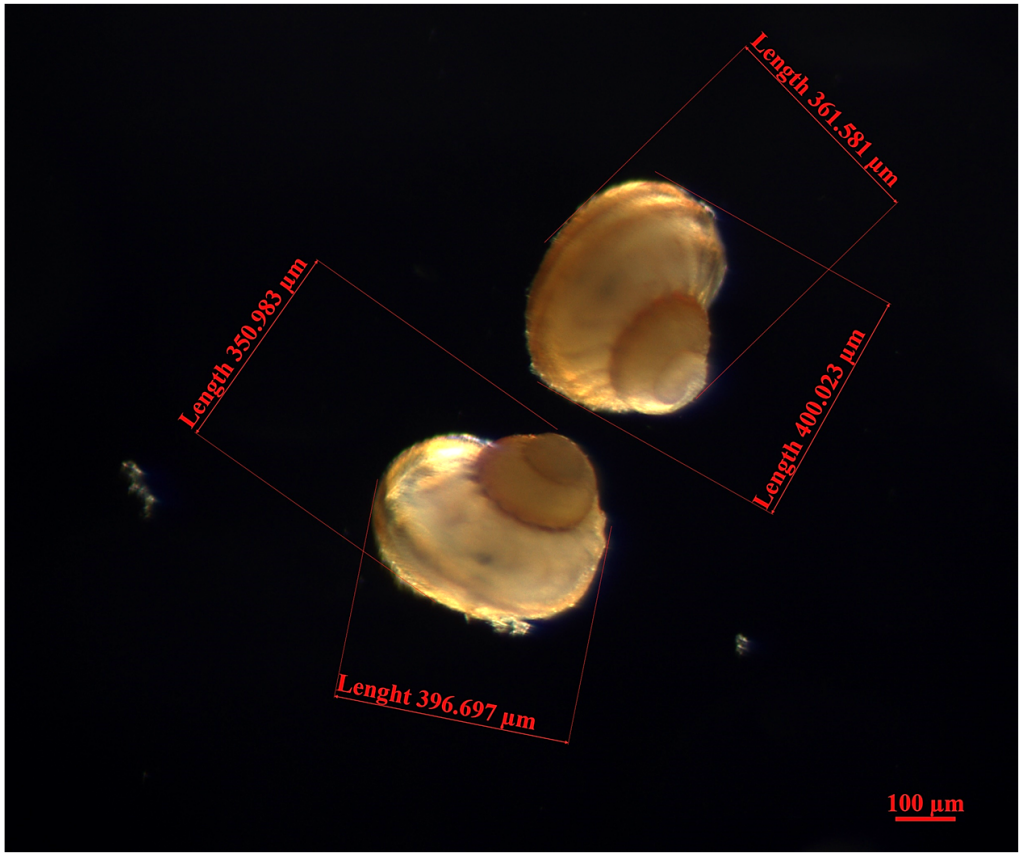

Figure 2. Microscopic photographs of *Lophocochlias parvissimus* larvae collected at Station A (2018) and OVF (2019). The scale bar indicates 100 µm.

The morphology of the *L. parvissimus* specimens retrieved in this study had the same features as previously described by Hedley (1899). The shell was solid with a yellowish-cream color and four whorls, and the umbilicus was small and oblique. *L. parvissimus* are known to have minute but solid shells that are tall for the family; the protoconch is multispiral or paucispiral and brown or white; the keel is a strong acute spiral, and the color is translucent white [9,15]. The specimen's morphology was similar to that represented in the microscopic photograph image of KimMoll18, WAM S94346, depicted in Figure 4B of Middelfart et al. (2020), who sampled the organism from the shallow marine environments of the tropical Kimberley region, Western Australia. According to Middelfart et al. (2020), *L. parvissimus* was the second most common species after *Parashiela* cf. *invisibilis* [12]. Also, the morphological characteristics of *L. parvissimus* resembled photographs of *L. minutissimus* in Figure 1A–H of Rubio and Rolán (2015). The diameter of *L. minutissimus* ranged from 0.84 to 1.08 mm (mean: 0.96 mm) in their study, which was approximately 2.4 times larger than the specimen of *L. parvissimus* (mean: 0.40 mm) described in this study. From the size of the *L. parvissimus* specimens, we can assume that they are larvae that may have dispersed from the nearby seabed in this study.

Lophocochlias parvissimus is subtidal and is commonly found in sediments to a depth of 30 m in tide pools around the bases of seaweeds [10,11]. The species of *Lophocochlias* are known to be intertidal, and their bathymetric range is between 0 and 60 m [15]. The specimens found in greater depths of deep water might have occurred due to the dragging effect of surrounding currents [15]. The geographical distribution is broad, and they can colonize on all types of substrates, including hard and soft bottoms such as rocky, sandy, and muddy bottoms with corals and coarse sand [15]. The planktotrophic larvae of *Lophocochlias* are free-living and, in the adult period, are not reported to be commensal with burrowing invertebrates. They are an epifaunal species that feed on detritus [11]. Interestingly, *L. parvissimus* was observed in the open ocean (Station A and OVF), approximately 1500 km away from the small islands of Seychelles, Mauritius, and Reunion and 2200 km away from the larger islands of Madagascar and Sri Lanka. Two assumptions can be made from the results of this study. First, it may be possible that *L. parvissimus* may live in the deep sea, represented by a bottom depth of 1429–2111 m at our study sites. Second, it is more likely that the larvae of *L. parvissimus* may be dispersed from coastal areas of nearby islands to the upper 100~200 m of the study sites by complex surface currents in the western Indian Ocean. This species is distributed across the majority of the Indo-Pacific region, including islands of the Pacific such as Hawaii, Kiribati, New Caledonia, the Loyalty Islands, Vanuatu, Fiji, Papua New Guinea, the Philippines, French Polynesia, and islands of the Indian Ocean, such as Madagascar, Reunion, and the western part of Australia [12–14,16,32–35], and from the open ocean along the Central Indian Ridge of the southwestern Indian Ocean in the present study.

This study generated a dataset of 353,133,548 raw reads through Illumina paired-end sequencing from *L. parvissimus*. A stringent quality filtering procedure, defined by a Phred quality score greater than 20 (see the Material and Methods section), was employed. As a result, we retained 342,701,216 filtered reads, which comprised 97.05% of the initial dataset. Subsequently, these filtered reads were utilized to assemble the mitochondrial genome of *L. parvissimus*.

Here, we have generated the first mitochondrial genome of the Tornidae species. The mitochondrial genome of *L. parvissimus* is 13,575 bp in length and contains 36 genes, including 13 PCGs (COX1, COX2, COX3, CYTB, ND1, ND2, ND3, ND4, ND4L, ND5, ND6, ATP6, and ATP8), 2 rRNAs (s-rRNA and l-rRNA), and 18 tRNAs (Figure 3). However, four tRNA genes were absent in the mitochondrial genome of *L. parvissimus*. This was because the genomic materials were extracted from small-sized larvae, potentially imposing limitations on obtaining sufficient mitogenomes for assembly. The overall base composition of the mitochondrial genome was 36.57% (A), 25.28% (T), 21.34% (C), and 16.8% (G). The proportion of A + T (61.85%) was ~1.62 times higher than that of G + C (38.14%).

To elucidate phylogenetic relationships, we attempted to utilize the mitochondrial protein-coding genes. When constructing phylogenetic trees, it is usually more informative to choose several genes from across species and families rather than a single gene. However, the lack of complete mitochondrial genome sequences in the family Tornidae hindered the use of the 13 protein-coding genes. As an alternative approach, we used COX1 to construct a phylogenetic hypothesis. Nevertheless, this study is significant in providing the first mitochondrial sequence of *L. parvissimus* in the Tornidae, elucidating the taxonomic relationship at the genus level. *L. minutissimus* (GenBank accession No. LC598190) is currently accepted as *L. parvissimus* in WoRMS, and tree topology indicates species identity (Figure 4). A similarity search using blastn showed 99.04% identity between *L. minutissimus* and *L. parvissimus*, suggesting that they are conspecific. Our data indicated monophyly of Tornidae with strong support (BS = 100%, BPP = 1) and implied a sister-group relationship between Tornidae and Caecidae (BS = 62%, BPP = 0.9). Also, the phylogenetic tree robustly demonstrates nodal supports within the family (BS $\geq$ 86%, BPP = 1), excluding Tateidae (BS = 53%, BPP = 0.9).

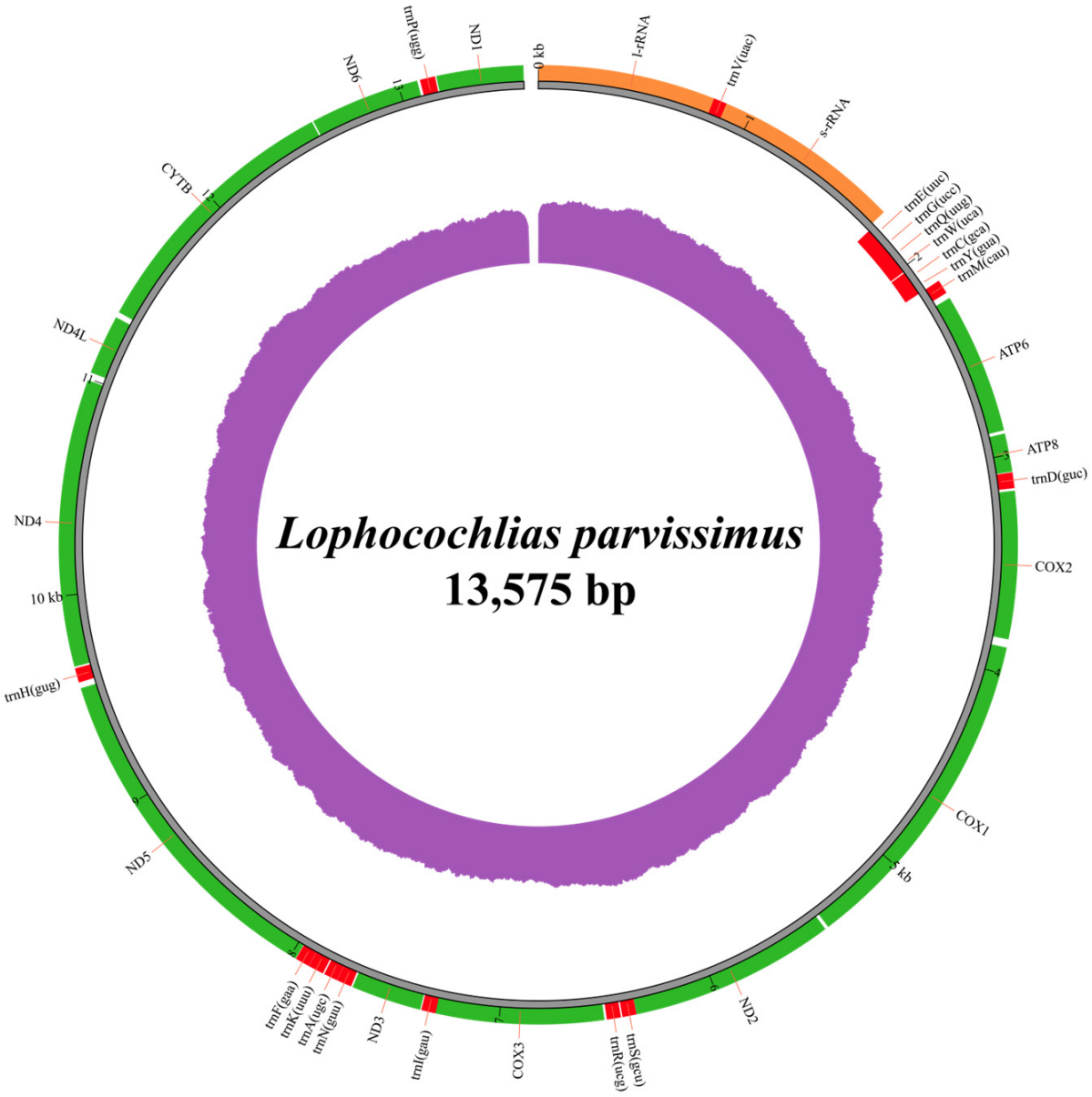

Figure 3. Map of the *Lophocochlias parvissimus* mitochondrial genome. The inner (purple) and outer circles represent sequencing depth and gene arrangement, respectively. In the outer circle, 13 PCGs are marked in green, 2 rRNA genes are colored in orange, and 18 tRNA genes are denoted in red.

In Figure 5, we found that the gene order remains consistent among six species belonging to the Littorinimorpha and Neogastropoda groups, except for *L. parvissimus*. Notably, the mitochondrial genome of *L. parvissimus* presents a distinctive modification in the syntenic arrangement involving the translocation of the ND3 and COX3 genes. However, the lack of comparative data makes it challenging to ascertain whether other species of *Lophocochlias* also exhibit this characteristic of gene relocation. Therefore, further studies are needed to incorporate additional mitochondrial data from Tornidae species to reconstruct a robust phylogenetic tree. Also, the utilization of 13 PCGs continues to be essential for achieving this objective.

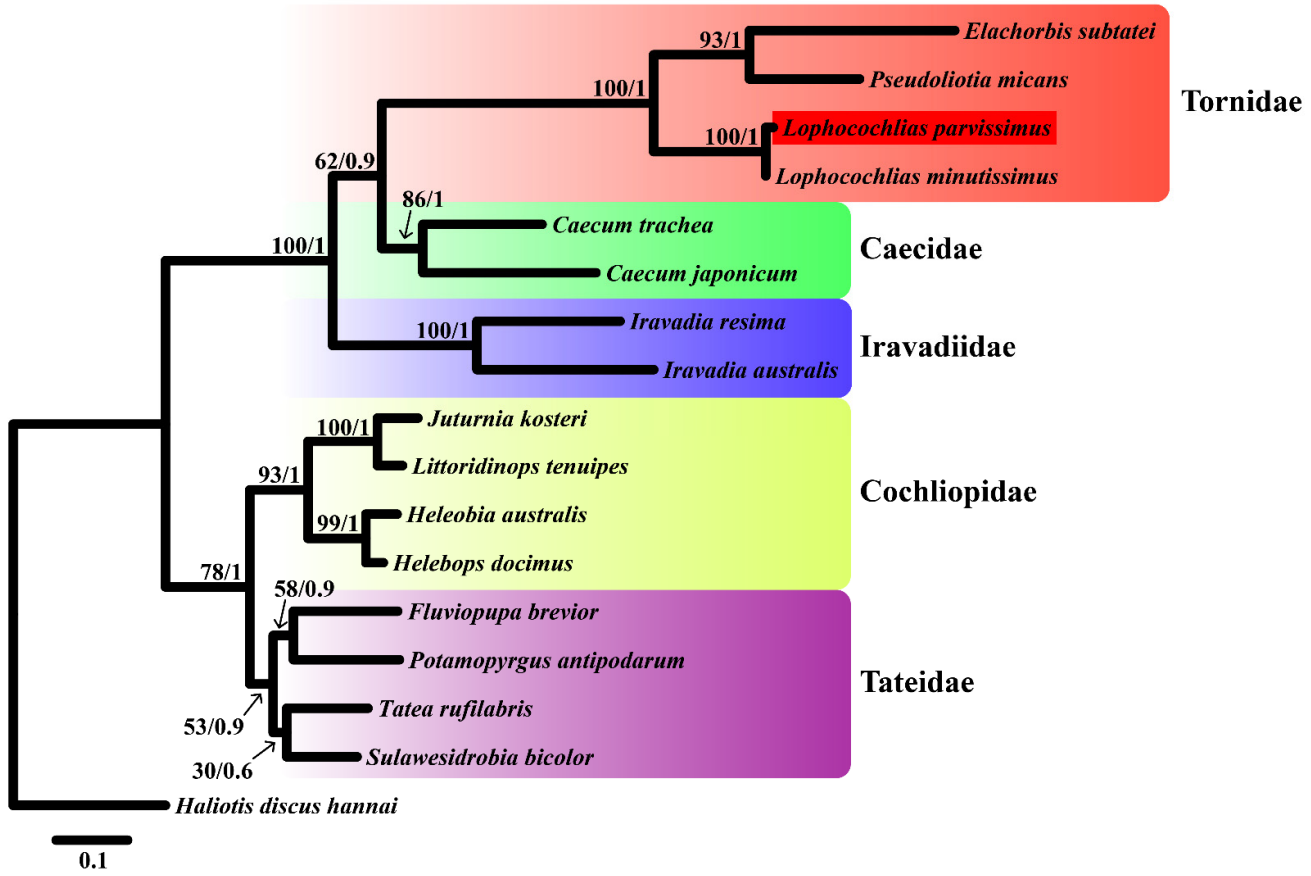

Figure 4. Maximum likelihood (ML) tree of the five families in Truncatelloidea using mitochondrial cytochrome c oxidase subunit I (COX1) sequences. The numbers on each node represent the bootstrap support values (BS) from ML and Bayesian posterior probabilities (BPP) from Bayesian inference (BI). The scale bar represents the number of substitutions per site.

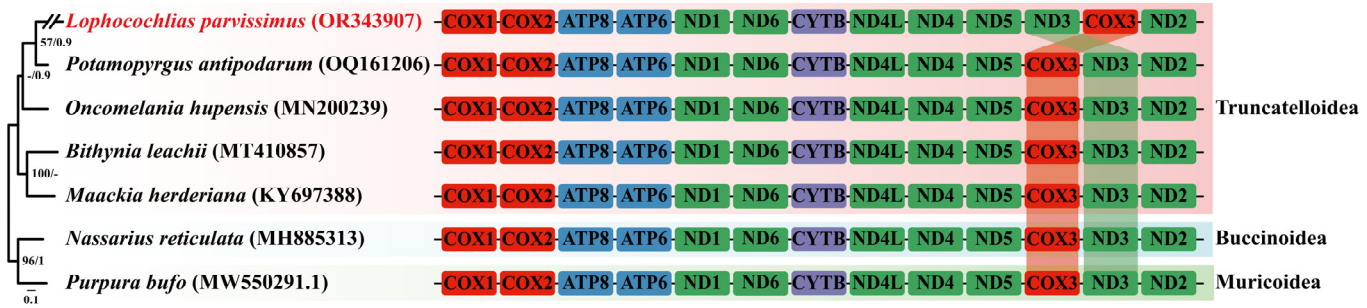

Figure 5. The maximum likelihood (ML) tree was reconstructed based on 13 protein-coding genes (PCGs). We used seven mitochondrial genomes from Littorinimorpha and Neogastropoda. Two species from Neogastropoda (*Nassariidae Reticulata* and *Purpura bufo*) were used as the outgroup. The numbers on each node represent the bootstrap support values (BS) from ML and Bayesian posterior probabilities (BPP) from Bayesian inference (BI). The scale bar under the ML tree represents the number of substitutions per site. The mitochondrial gene arrangement was overlaid onto the ML tree. Measurements of the complete mitochondrial DNA length and the lengths of individual PCGs were not conducted in this result.

4. Conclusions

Lophocochlias parvissimus were found in the epipelagic zones at Station A and OVF in the Central Indian Ridge. We conducted a comprehensive investigation into the ecological and molecular characteristics of *L. parvissimus* larvae and presented the first mitochondrial genome in the family Tornidae. Based on COX1, we constructed ML and BI trees to unveil the evolutionary and phylogenetic relationships of *L. parvissimus* larvae. Through our study, we discovered Tornidae forms a monophyletic group encompassing three genera: *Lophocochlias*, *Pseudoliotia*, and *Elachorbis*. Notably, we made a remarkable discovery during our investigation. The larvae of *L. parvissimus* were unexpectedly found in the upper 100–200 m of the epipelagic zone in the Central Indian Ridge at Station A and OVF. This finding suggests that the larvae might have been dispersed from nearby coastal areas in the Indian Ocean to offshore waters. Our study provided significant insight into *L. parvissimus* and its relationship within the family Tornidae. However, obtaining the whole mitochondrial genomes of other Tornidae species is required in future research to ensure a more robust and reliable phylogenetic study.

Author Contributions: Conceptualization, S.-i.E. and J.-H.K.; methodology, M.K., H.C., H.K. and J.K.; formal analysis, M.K., H.C., H.K., J.K. and H.G.J.; data curation, M.K., H.C., H.K. and H.G.J.; writing—original draft preparation, M.K., H.C., S.-i.E. and J.-H.K.; writing—review and editing, M.K., H.C., S.-i.E. and J.-H.K.; project administration, J.-H.K. All authors have read and agreed to the published version of the manuscript.

Funding: This research was a part of the project titled "Understanding the deep-sea biosphere on seafloor hydrothermal vents in the Indian Ridge (No. 20170411)" funded by the Ministry of Oceans and Fisheries, Korea. This research was also supported by the Management of Marine Bio-resources and Systematic Research (MABIK 2023M00200) funded by the National Marine Biodiversity Institute of Korea and the Chung-Ang University Research Scholarship Grants in 2023.

Institutional Review Board Statement: Not applicable.

Informed Consent Statement: Not applicable.

Data Availability Statement: The mitochondrial sequence of *Lophocochlias parvissimus* is openly available from the GenBank of NCBI (https://www.ncbi.nlm.nih.gov, accessed on 30 October 2023) under accession No. OR343907.

Conflicts of Interest: The authors declare no conflict of interest.

References

1. Günther, C.-P. Dispersal of intertidal invertebrates: A strategy to react to disturbances of different scales? *Neth. J. Sea Res.* **1992**, *30*, 45–56. [CrossRef]
2. Baco, A.R.; Etter, R.J.; Ribeiro, P.A.; Von der Heyden, S.; Beerli, P.; Kinlan, B.P. A synthesis of genetic connectivity in deep-sea fauna and implications for marine reserve design. *Mol. Ecol.* **2016**, *25*, 3276–3298. [CrossRef] [PubMed]
3. Lutz, R.A.; Kennish, M.J. Ecology of deep-sea hydrothermal vent communities: A review. *Rev. Geophys.* **1993**, *31*, 211–242. [CrossRef]
4. Lalli, C.M.; Gilmer, R.W. *Pelagic Snails: The Biology of Holoplanktonic Gastropod Mollusks*; Stanford University Press: Redwood City, CA, USA, 1989.
5. Kim, M.; Kang, J.-H.; Kim, D. Holoplanktonic and meroplanktonic larvae in the surface waters of the Onnuri Vent Field in the Central Indian Ridge. *J. Mar. Sci. Eng.* **2022**, *10*, 158. [CrossRef]
6. Mills, S.W.; Beaulieu, S.E.; Mullineaux, L.S. *Photographic Identification Guide to Larvae at Hydrothermal Vents*; Woods Hole Oceanographic Institution: Falmouth, MA, USA, 2009.
7. MolluscaBase, Eds. MolluscaBase. *Lophocochlias parvissimus* (Hedley, 1899). Accessed through: World Register of Marine Species. 2023. Available online: https://www.marinespecies.org/aphia.php?p=taxdetails&id=765226 (accessed on 15 February 2023).
8. WoRMS. World Register of Marine Species. 2023. Available online: https://www.marinespecies.org (accessed on 20 February 2023).
9. Hedley, C. The Mollusca of Funafuti, part 2, Pelecypoda and Brachiopoda. *Aust. Mus. Mem.* **1899**, *3*, 489–535. [CrossRef]
10. Kay, E.A. Molluscan distribution patterns at Canton Atoll. *Atoll Res. Bull.* **1978**, *221*, 159–170.
11. Rubio, F.; Fernández-Garcés, R.; Rolán, E. The genus *Haplocochlias* (Gastropoda: Skeneidae). *Iberus* **2013**, *31*, 41–126.

12. Middelfart, P.; Kirkendale, L.; Bryce, C. Smaller molluscs from a multi-taxon survey (2012–2014) of the shallow marine environments of the tropical Kimberley region, Western Australia. *Rec. Aus. Mus.* **2020**, *85*, 117–183. [CrossRef]
13. Kay, E.A.; Switzer, M.F. Molluscan distribution patterns in Fanning Island Lagoon and a comparison of the mollusks of the lagoon and the seaward reefs. *Pac. Sci.* **1974**, *28*, 275–295.
14. Pilsbry, H.A. Revision of WM Gabb's Tertiary Mollusca of Santo Domingo. *Proc. Acad. Nat. Sci. Phila.* **1921**, *73*, 305–435.
15. Rubio, F.; Rolán, E. The genus *Lophocochlias* Pilsbry, 1921 (Gastropoda, Tornidae) in the Indo-West Pacific. *Novapex* **2015**, *16*, 105–120.
16. Maes, V.O. The littoral marine mollusks of Cocos-Keeling Islands (Indian Ocean). *Proc. Acad. Nat. Sci. Phila.* **1967**, *119*, 93–217.
17. Javonillo, R.; Malabarba, L.R.; Weitzman, S.H.; Burns, J.R. Relationships among major lineages of characid fishes (Teleostie: Ostariophysi: Characiformes), based on molecular sequence data. *Mol. Phylogenet. Evol.* **2010**, *54*, 498–511. [CrossRef] [PubMed]
18. Hiesel, R.; von Haeseler, A.; Brennicke, A. Plant mitochondrial nucleic acid sequences as a tool for phylogenetic analysis. *Proc. Natl. Acad. Sci. USA* **1994**, *91*, 634–638. [CrossRef] [PubMed]
19. Strüeder-Kypke, M.C.; Lynn, D.H. Comparative analysis of the mitochondrial cytochrome c oxidase subunit I (COI) gene in ciliates (Alveolata Ciliophora) and evaluation of its suitability as a biodiversity marker. *Syst. Biodivers.* **2010**, *8*, 131–148. [CrossRef]
20. Kim, J.; Son, S.-K.; Kim, D.; Pak, S.-J.; Yu, O.H.; Walker, S.L.; Oh, J.; Choi, S.K.; Ra, K.; Ko, Y. Discovery of active hydrothermal vent fields along the Central Indian Ridge, 8–12°S. *Geochem. Geophys.* **2020**, *21*, e2020GC009058. [CrossRef]
21. Hood, R.R.; Beckley, L.E.; Wiggert, J.D. Biogeochemical and ecological impacts of boundary currents in the Indian Ocean. *Prog. Oceanogr.* **2017**, *156*, 290–325. [CrossRef]
22. Parsons, T.R.; Maita, Y.; Lalli, C.M. *A Manual of Chemical and Biological Methods for Seawater Analysis*; Pergamon Press: Oxford, UK, 1984.
23. Martin, M. Cutadapt removes adapter sequences from high-throughput sequencing reads. *EMBnet. J.* **2011**, *17*, 10–12. [CrossRef]
24. Jeon, M.S.; Jeong, D.M.; Doh, H.; Kang, H.A.; Jung, H.; Eyun, S. A practical comparison of the next-generation sequencing platform and assemblers using yeast genome. *Life Sci. Alliance* **2023**, *6*, e202201744. [CrossRef]
25. Meng, G.; Li, Y.; Yang, C.; Liu, S. MitoZ: A toolkit for animal mitochondrial genome assembly, annotation and visualization. *Nucleic Acids Res.* **2019**, *47*, e63. [CrossRef]
26. Krzywinski, M.; Schein, J.; Birol, I.; Connors, J.; Gascoyne, R.; Horsman, D.; Jones, S.J.; Marra, M.A. Circos: An information aesthetic for comparative genomics. *Genome Res.* **2009**, *19*, 1639–1645. [CrossRef] [PubMed]
27. Katoh, K.; Misawa, K.; Kuma, K.; Miyata, T. MAFFT: A novel method for rapid multiple sequence alignment based on fast Fourier transform. *Nucleic Acids Res.* **2002**, *30*, 3059–3066. [CrossRef] [PubMed]
28. Minh, B.Q.; Schmidt, H.A.; Chernomor, O.; Schrempf, D.; Woodhams, M.D.; Von Haeseler, A.; Lanfear, R. IQ-TREE 2: New models and efficient methods for phylogenetic inference in the genomic era. *Mol. Biol. Evol.* **2020**, *37*, 1530–1534. [CrossRef] [PubMed]
29. Lanfear, R.; Frandsen, P.B.; Wright, A.M.; Senfeld, T.; Calcott, B. PartitionFinder 2: New methods for selecting partitioned models of evolution for molecular and morphological phylogenetic analyses. *Mol. Biol. Evol.* **2016**, *34*, 772–773. [CrossRef] [PubMed]
30. Kozlov, A.M.; Darriba, D.; Flouri, T.; Morel, B.; Stamatakis, A. RAxML-NG: A fast, scalable and user-friendly tool for maximum likelihood phylogenetic inference. *Bioinformatics* **2019**, *35*, 4453–4455. [CrossRef] [PubMed]
31. Ronquist, F.; Teslenko, M.; van der Mar, P.; Ayres, D.L.; Darling, A.; Hohna, S.; Larget, B.; Liu, L.; Suchard, M.A.; Huelsenbeck, J.P. MrBayes 3.2: Efficient Bayesian phylogenetic inference and model choice across a large model space. *Syst. Biol.* **2012**, *61*, 539–542. [CrossRef]
32. Kay, E. The littoral marine molluscs of Fanning Island. *Pac. Sci.* **1971**, *25*, 260–281.
33. Okutani, T. *Marine Mollusks in Japan*; Tokai University Press: Tokyo, Japan, 2000.
34. Higo, S.; Callomon, P.; Goto, Y. *Catalogue and Bibliography of the Marine Shell-Bearing Mollusca of Japan*; Elles Scientific Publications: Osaka, Japan, 1999.
35. Fukuda, H. Marine gastropoda (Mollusca) of the Ogasawara (Bonin) Islands. Part 3: Additional records, marine Mollusks in Japan. *Ogasawara Res.* **1995**, *21*, 1–142.